AIAA JOURNAL
Vol. 35, No. 6, June 1997

Experiments on Impulsively Started Jet Diffusion Flames

H. Johari,* K. J. Desabrais,† and J. C. Hermanson*
Worcester Polytechnic Institute, Worcester, Massachusetts 01609

The starting vortex of an impulsively generated jet diffusion flame was studied experimentally. Fuel jets were produced by the sudden discharge via a solenoid valve into still air. The fuel jet was ignited by a pilot flame. The length and lateral spread of the flame were determined by video imaging. All flames were in the buoyancy-driven regime after the starting transient. The height at which the starting vortex burned off completely was approximately the same as the mean flame length of the subsequent steady flame. The penetration of the flame tip associated with the starting vortex can be correlated by a buoyancy parameter derived from the isothermal starting plume theory of Turner. An unexplained dependence of penetration on nozzle diameter was observed. The timescale for the mixing of the starting vortex at its maximum flame height appears to be about one-half of the vortex rotation time at the same location. These findings may be useful in understanding unsteady combustion phenomena, especially as they pertain to active combustion control schemes.

Introduction

THERE is renewed interest in unsteady flowfields, mainly from the perspective of active flow control. The general notion has been that by forcing any flow at an appropriate frequency and at relatively low amplitudes, the flow characteristics, such as instability and mixing, can be significantly modified. These ideas stem from observations of the alteration of coherent structures in shear layers when the flow is forced at the subharmonic of the natural shedding frequency.[1] The shear layer growth can be effectively arrested or augmented when the forcing is applied near the splitter plate tip. Application of forcing in isothermal jets has also increased the near-field entrainment and spreading rates even though the steady jet characteristics are generally recovered in the far field.[2]

Another area where unsteady flows play a dominant role is in pulsed combustion and combustion control. The effects of pulsing on jet diffusion flames have been studied by Lovett and Turns.[3] At low frequencies and substantial amplitudes, the flame length was modestly reduced in comparison with the steady jet flame length. Numerous other studies have dealt with the acoustic, or small amplitude, pulsing of flames. However, there appear to be few studies that have addressed the effects of the most fundamental forms of unsteadiness on reacting jets, such as the delta- and step-function flow discharges corresponding to individual turbulent puffs and impulsively started jets, respectively.

A previous series of experiments on discrete, impulsively generated reacting puffs showed that the puffs mixed and burned very quickly.[4] This was manifested by a shorter observed flame length of puffs compared with steady jets. The faster mixing rate was presumed to be due to the high entrainment rate of individual turbulent puffs. Experiments and modeling of impulsively started isothermal jets showed that the starting vortex follows the same scaling (i.e., mean velocity with axial position) as that of the steady jet and that its penetration scales with the square root of time.[5–7] Moreover, the starting vortex has been found to mix faster than the rest of the jet in aqueous flows. The present study was undertaken to explore the extent to which similar phenomena may occur in impulsively started jets with chemical reaction and heat release.

The aim of the current project was to investigate the mixing, penetration, and spreading rate of the starting vortex in jet diffusion flames. Understanding the fundamental effects of this most simplified form of unsteadiness on mixing and combustion may shed light on the more complicated practical problems of pulsed combustors and active control of combustion.

Received June 1, 1996; revision received Jan. 8, 1997; accepted for publication Feb. 19, 1997.

*Associate Professor, Mechanical Engineering Department. Senior Member AIAA.

†Graduate Student, Mechanical Engineering Department.

Experimental Details

Apparatus

The study of impulsively started diffusion flames required an apparatus that allowed for a very rapid discharge of fuel at a steady velocity from a nozzle. The experimental apparatus described here is shown schematically in Fig. 1. The entire apparatus was placed on a square platform of 1.4 m on each side, which was set 30 cm above the laboratory floor. The experiment was surrounded by four screens, each 1.2 × 1.2 m in size, to reduce any drafts in the vicinity of the flowfield.

The primary components of the apparatus were a contoured nozzle, a solenoid valve, and a sharp-edged orifice plate section for volumetric flow measurements under steady conditions. The orifice plate diameter was 5.1 mm. An accumulator with a volume of 800 cm^3 was placed between the orifice plate and the solenoid valve to suppress potential oscillations in the nozzle velocity during the impulsive start. The experiment used two different nozzles with exit diameters of 9.9 and 6.4 mm and area contraction ratios of 6.6:1 and 16:1, respectively. The nozzles were made of brass and the contours were designed to produce top-hat velocity profiles at the exit. A screen and honeycomb flow straightener were used after the solenoid valve to ensure uniform flow entering the nozzle contraction. The solenoid valve had an internal diameter of 2.4 mm and an opening time of about 20 ms (manufacturer's specification). The flow velocity was regulated by a needle valve and the maximum flow rate was limited by the available fuel line pressure of about 30 cm of water.

The fuel used in the present experiment was city gas with a specific gravity of 0.579. The primary constituents of the fuel were methane, ethane, nitrogen, and carbon dioxide with volumetric concentrations of 96.1, 1.9, 1.0, and 0.6%, respectively. The remaining 0.4% was composed of trace species. The fuel was ignited with a small pilot flame positioned at the edge of the nozzle exit diameter. Steady jet flames did not lift off except at the highest flow rates with the 6.4-mm-diam nozzle; thus, no flameholder was required. The combustion products were disposed of by a low-flow-rate fume hood centered above the apparatus.

The flow rate for the steady jet flames was adjusted to the desired level by using the primary flow control (needle) valve and measuring the pressure drop across the orifice plate with a manometer. For each nozzle, two different flow rates were employed. The steady-state operating conditions, such as the nozzle exit diameter d and the mean exit velocity U_0, for the four cases studied in the present experiments are summarized in Table 1.

The flow was initiated when the solenoid valve was energized by manually activating an electronic control circuit. A hot-wire

Table 1 Summary of experimental conditions

Case	d, mm	U_0, m/s	$Re_0 \equiv U_0 d/\nu_0$
1	9.9	8.9	5500
2	9.9	5.5	3400
3	6.4	13.3	5300
4	6.4	8.5	3400

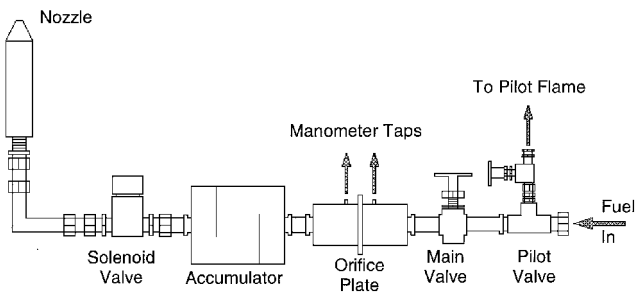

Fig. 1 Schematic sketch of experimental apparatus.

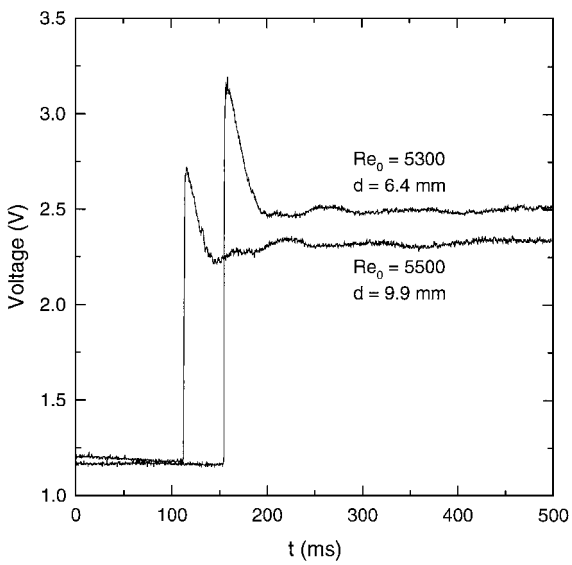

Fig. 2 Time traces of raw hot-wire voltage for cases 1 and 3.

anemometer was utilized to evaluate the flow quality and the rise time of the velocity at the nozzle exit for the case of nonreacting flow (i.e., no ignition source). The hot wire was placed within half a nozzle diameter downstream of the nozzle exit. The anemometer output voltage was sampled at 6 kHz for 0.5 s. Five test runs were recorded for each case. Sample voltage traces for cases 1 and 3 are shown in Fig. 2. At first, the voltage increased to a peak value that was 30–40% greater than the mean value before decreasing to a steady level. The time history of the starting flow is quite similar among all four cases, as is evident in Fig. 2 for cases 1 and 3. The time it takes the velocity to reach its steady value varied between 100 and 150 ms, corresponding to about four video frames. The initial overshoot was greater for the smaller nozzle and is believed to be because of the presence of the accumulator in the setup. Operating without the accumulator, however, produced velocity time traces having a few oscillation cycles. These oscillations were confined to the first 100 ms of each run. Experiments conducted with and without the accumulator resulted in mean flame lengths and starting vortex penetration rates that were in quantitative agreement, to within our experimental uncertainty.

Measurements

The flames were recorded by an HI-8 camcorder and a charge-coupled device camera at 30 frames per second with exposure times of 10 and 8 ms, respectively. The recorded images of the luminous

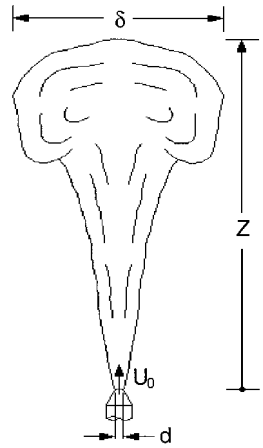

Fig. 3 Definition of measured quantities for the impulsively started jet flame.

portions of the flame reflect the radiating soot particles, which are closely associated with the local stoichiometric surfaces.[8] Thus, the outline of the visible flame corresponds roughly with the outermost reaction surface. For each of the four cases, 25 runs were recorded and then data from a selected subset were analyzed frame by frame to arrive at the temporal evolution of the impulsively started jet flame. The framing rate of 30 per second provided sufficient resolution for the present low-speed flows and resulted in a temporal uncertainty of $\pm$17 ms. The uncertainty in length measurements was estimated at $\pm$2.5 cm, primarily because of errors associated with determination of the position of flame edges.

Measurements of the height of the burning vortex tip Z and the maximum burning vortex width δ are reported here. After the burnoff of the starting vortex, the height of the oscillating flame tip was used to calculate the mean flame length L. The small run-to-run variations in the time origin of the flow precluded the use of ensemble averaging of the flame-tip data. The schematic of the starting vortex and the ensuing jet in Fig. 3 define the quantities measured.

Results and Discussion

After flow initiation, a large-scale toroidal vortex was formed and the rest of the jet followed this vortex. As the vortex convected in the vertical direction, the overall structure of the flow (i.e., starting vortex and the ensuing jet) was maintained until all of the fuel within the starting vortex was oxidized and all luminous soot was consumed. A set of digitized images from a case 1 run is shown in Fig. 4, where the boundary of luminous flame was extracted by using edge detection routines of image processing software. The line near the bottom of each image indicates the nozzle exit plane; the time since flow initiation is provided below each image. The axial extent in these images is approximately 100 nozzle diameters. The blue flames near the nozzle exit were barely detectable by the video camera and were subsequently removed by the thresholding process during image processing. The last three images in the set are successive images immediately before the starting vortex burning out. The starting vortex in this case was completely consumed within 15 video frames, corresponding to an elapsed time of about 0.5 s. After the starting vortex had completely reacted (as in the last image), the jet tip assumed an arrowhead shape and moved past the location where the starting vortex was last visible, ultimately leading to the establishment of an oscillating flame tip.

For each run, the position of the tip of burning vortex Z was recorded as a function of time from flow initiation. Temporal evolution of the starting vortex and the stationary flame tip position is shown in Fig. 5 for one run from each of the four cases. The data in Fig. 5a correspond to the run imaged in Fig. 4. The first portion of each run is associated with the ascent of the starting vortex and the remaining portion indicates the oscillatory nature of the flame tip when the mean flow had achieved steady state. The starting vortex completely reacted just after it had reached its maximum penetration. It might be expected that after passage of the starting vortex and burnoff of the jet region immediately behind it, the mean flow would attain a stationary nature. This is verified by the presence of instantaneous flame tip fluctuations, which become

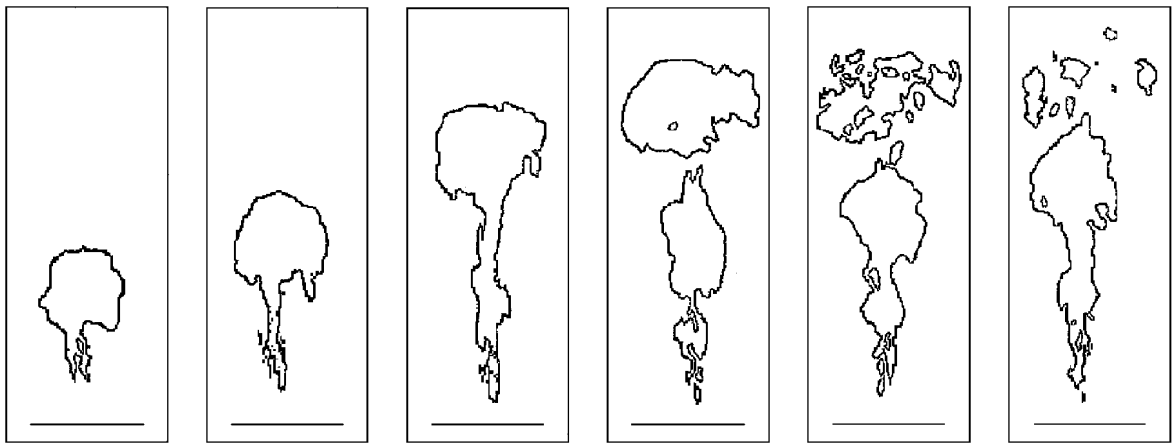

$t = 0.17$ s $t = 0.23$ s $t = 0.37$ s $t = 0.43$ s $t = 0.47$ s $t = 0.50$ s

Fig. 4 Digitized images of the starting vortex progression and burnoff for case 1 ($d = 9.9$ mm and $Re_0 = 5.5 \times 10^3$).

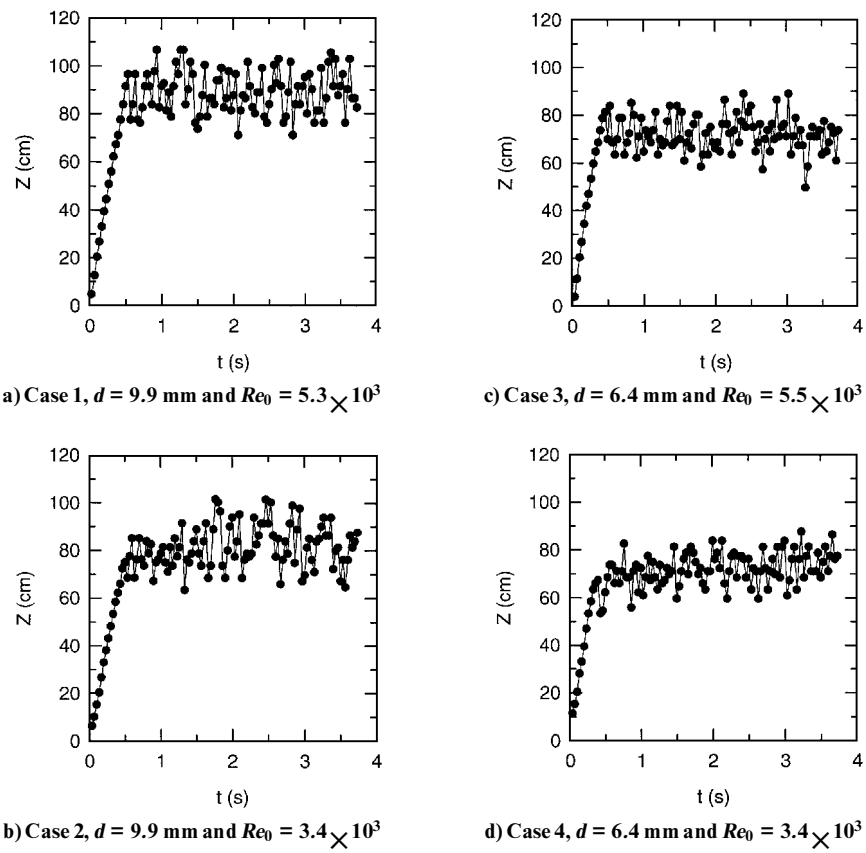

a) Case 1, $d = 9.9$ mm and $Re_0 = 5.3 \times 10^3$

c) Case 3, $d = 6.4$ mm and $Re_0 = 5.5 \times 10^3$

b) Case 2, $d = 9.9$ mm and $Re_0 = 3.4 \times 10^3$

d) Case 4, $d = 6.4$ mm and $Re_0 = 3.4 \times 10^3$

Fig. 5 Temporal evolution of the flame tip.

consistent with steady jet fluctuations after a few cycles. The oscillations of the flame tip have been explained in terms of the large-scale structure of the underlying jet flow by Dahm and Dimotakis[9] in isothermal reacting jets and by Mungal et al.[10] in buoyancy- and momentum-driven diffusion flames. The frequency of flame-tip oscillations has been shown to scale with the passage time of the jet large-scale structures at the location of the mean flame length.

The maximum recorded height of the luminous starting vortex is referred to as the vortex flame height. This height was always within 10% of the mean flame length of the stationary jet, as determined from about 100 instantaneous flame images after establishment of the steady jet. If the flame height is assumed to be an indication of the mixing rate and fuel consumption, i.e., shorter flame heights indicating faster mixing rate and combustion, then the comparable flame heights of the vortex and the steady jet imply that fuel within the vortex is approximately consumed to the same extent as in the steady jet at the same distance above the nozzle. Alternatively, the diffusion flame structure can be regarded as consisting of a large number of strained flame elements that separate the fuel and oxidizer.[11] This implies that the combustion will cease only when the fuel is completely consumed locally[12] unless the local strain rate is sufficiently high to quench the flame.[13] This quenching is unlikely for the strain rates near the tip of the starting vortex in this experiment.

The time required to complete the burnoff of starting vortex, i.e., the time it took from the first observation of incipient burnoff to total burnoff of the starting vortex, was estimated from the video recordings. The burnoff times were approximately two or three frames (corresponding to 70–100 ms) for all four cases. The vortex turnover time, calculated from the local width divided by the local velocity at the vortex flame height, was about twice as large as these burnoff times. This suggests that, within one vortex revolution of this flowfield, all of the vortex material becomes mixed to at least the stoichiometric ratio. The timescale for the burnoff is in agreement with the Broadwell and Breidenthal[14] model for mixing in shear

Table 2 Summary of stationary flame parameters

Case	L/d	ξ_L	Re_L	Ri_s
1	88 ± 10	11.3	21,600	9.3×10^{-4}
2	83 ± 9	14.6	14,200	2.4×10^{-3}
3	115 ± 13	9.7	16,000	2.7×10^{-4}
4	116 ± 11	13.3	10,000	6.6×10^{-4}

flows. Furthermore, Johari et al.[7] have made similar observations in aqueous, isothermal reacting jets where the timescale for the complete reaction within the starting vortex was proportional to the local large timescale.

Stationary Jet Flame Length

The instantaneous flame-tip heights, following the passage of the starting vortex, were averaged for the stationary portion of each run (typically 3 s) and the average value was labeled the mean flame length for that run. A number of runs from each case were then averaged to arrive at the mean flame length, L, for that case. These mean flame lengths are shown in Table 2 along with several related parameters discussed below. The standard deviation of the fluctuating flame-tip height was about 10% of the mean flame length in each run and the variations of the mean flame length among different runs for each case were less than 5%.

To determine whether the stationary portion of the flow was momentum or buoyancy driven, the parameter $\xi_L \equiv Ri_s^{1/3}\,(L/D_s)$ developed by Becker and Yamazaki[15] was utilized. The source Richardson number Ri_s and the source diameter D_s are defined as follows:

$$Ri_s = g D_s / U_s^2 \tag{1}$$

and

$$D_s = \left(\frac{4M}{\pi \rho_\infty U_s^2} \right)^{\frac{1}{2}} \tag{2}$$

where M, U_s, g, and ρ_∞ are, respectively, the mean source momentum flux, mean source velocity, gravitational acceleration, and ambient density. For a nozzle producing a top-hat velocity profile with uniform density ρ_0, the source velocity is equal to the mean nozzle velocity U_0 and the source diameter $D_s = d(\rho_0/\rho_\infty)^{1/2}$. Then ξ_L can be written in terms of the fuel specific gravity, nozzle diameter and velocity, and the mean flame length:

$$\xi_L = \left[(\rho_\infty/\rho_0)(gd/U_0^2) \right]^{\frac{1}{3}} (L/d) \tag{3}$$

According to Becker and Yamazaki,[15] flames with $\xi_L < 2$ are momentum driven, whereas those with $\xi_L > 10$ are buoyancy driven. Flames having ξ_L values in between these limits are transitional. The flames in the present study are buoyancy driven, as shown in Table 2.

A correlation for prediction of mean flame lengths based on the entrainment of jets was provided by Becker and Liang[16] for flames with $1 < \xi_L < 20$. The relation for the mean flame length L is given below for $Re_L > 8000$

$$(D_s \beta / LW)^{\frac{2}{3}} = 0.18 + 0.022\,\xi_L \tag{4}$$

where W is the mass fraction of fuel in a stoichiometric mixture with air and β is the square root of the adiabatic flame temperature, normalized by the ambient temperature, divided in turn by the molecular weight of the products, normalized by the molecular weight of air. The parameters W and β are equal to 0.0549 and 2.8, respectively, for methane; most hydrocarbon fuels have similar values. The flame Reynolds number was defined by Becker and Liang as

$$Re_L \equiv 11 \left(\frac{\rho_0 U_0 d}{\mu_\infty} \right) \left(\frac{\beta}{W} \right) \left(\frac{L}{d} \right)^{-1} \tag{5}$$

The values of source Richardson number Ri_s, ξ_L, and Re_L are shown in Table 2 for the four cases.

Because the classification used by Becker and Yamazaki[15] places the stationary portion of present flames in the buoyancy-driven regime, scaling arguments developed for isothermal momentum-driven starting jets[5–7] may not be applicable to the present flames. This is especially true in terms of the jet penetration that scales with the square root of time; the present data indicate that the penetration is more nearly linear with time. Delivery pressure limitations in the current setup precluded the creation of flames in the fully momentum-driven regime with $\xi_L < 2$. Conversely, flames with even greater buoyancy could be generated by lowering the nozzle velocity. However, this would lead to decreasing Re_0 below the point where fully turbulent flames exist.

The flow is initially momentum driven because of the impulsive nature of jet initiation. However, upon mixing with ambient air and subsequent combustion and heat release, the starting vortex becomes buoyancy driven in about 50 ms and at a distance of 7–10 cm (equivalent to $7d$–$15d$ for cases 2 and 3) from the nozzle. This corresponds to the first two data points in the plots of Fig. 5. Cases 2 and 3 were selected because they had the smallest and largest vortex celerities in the current experiments. The criterion for buoyancy domination within the starting vortex was determined by considering the starting vortex Richardson number, $Ri_v = (\rho_\infty - \rho_v) g \delta / \rho_v U_v^2$, where δ, ρ_v, and U_v are the starting vortex width, density, and celerity, respectively. The time and distance values cited earlier were calculated by finding the location at which the vortex Richardson number exceeded $\frac{1}{4}$. The vortex velocity and width values were obtained from the average penetration and spreading rates.

An implicit relation for the normalized mean flame length, L/d, can be obtained by combining Eqs. (3) and (4). The resulting equation can then be solved to give the expected values of L/d for the conditions of the current investigation. The calculated flame lengths are, on average, 17% higher than the actual mean measured values given in Table 2. This discrepancy, however, drops to less than 6% when the maximum observed values of flame length are considered. Because the flame lengths reported by Becker and Liang,[16] from which Eqs. (3) and (4) were obtained, were determined by visual observation only, it is perhaps to be expected that the longest flame lengths in our experiment will be more consistent with their empirical formulation than the average values. The cause of the remaining discrepancy might be related to the initial conditions. Specifically, the velocity profile in the nozzle in the current work (which used contracting nozzles) was different than that of Becker and Liang (who used a long, straight inlet port).

Starting Vortex Penetration

The tip location of the burning vortex Z was correlated with time t and the penetration of the starting vortex while burning appeared to scale nearly linearly with time (see Fig. 5). This allowed a least-squares line to be fit to Z/d vs tU_0/d. The correlation coefficients were about 90% or better for the majority of the analyzed runs. Furthermore, the slope of the line [denoted by $(dZ/dt)/U_0$] was quite repeatable among the various runs for each case. However, it varied significantly for the four different cases. These slopes, which can be interpreted as constant vortex tip speeds, are shown in Table 3. It was expected that these slopes should be, at the minimum, free of Reynolds number effects for a given nozzle diameter if not also nozzle diameter independent. This expectation is based on the observations of a constant celerity, equal to $0.12U_0$ and independent of Re_0, for the large-scale structures within steady jet diffusion flames.[10] The correlations in the current work indicate that the celerity of the burning vortex does depend on both the nozzle diameter and the Reynolds number for impulsively started jets. To consolidate the observed celerities among the four cases, other scalings were explored and one in particular is discussed in the following.

Table 3 Summary of coefficients used in scalings for the burning starting vortex

Case	Re_0	$(dZ/dt)/U_0$	k	Z_0/d	$d\delta/dZ$
1	5500	0.19 ± 0.010	5.4 ± 0.19	-2.5	0.37 ± 0.04
2	3400	0.29 ± 0.012	5.7 ± 0.18	-9.4	0.31 ± 0.04
3	5300	0.14 ± 0.007	6.7 ± 0.29	-17.1	0.30 ± 0.04
4	3400	0.21 ± 0.013	6.8 ± 0.41	-10.4	0.26 ± 0.02

As stated earlier, the tip of an isothermal, impulsively started, momentum-driven jet penetrates as the square root of time. It is unlikely that this isothermal jet scaling can be applied to the present burning, starting vortices. The scaling for a buoyancy-driven starting plume, however, may be able to correlate the data for the four cases studied in the present work. Turner[17] has developed a theory for the penetration and entrainment of the starting vortex in buoyancy-driven plumes in the Boussinesq limit, i.e., small density differences. The most important parameter in the theory is the buoyancy flux at the source $F \equiv (1 - \rho_0/\rho_\infty) g(\pi d^2/4) U_0$. The penetration of the starting vortex then scales with $(Ft^3)^{1/4}$. Because the $t^{3/4}$ approximates the fitted linear dependence for the short ($\sim$0.5 s) duration of the observations, it was thought that the starting plume theory of Turner may be able to account for the discrepancy in penetration rate (as a function of Reynolds number and nozzle diameter) among the data from different cases. As it turns out, the $t^{3/4}$ dependence provides an even better fit to the data than the linear fit considered earlier.

The only shortcoming of the application of the theory to the present measurements is that the initial buoyancy flux is quite small in comparison with the buoyancy flux within the burning starting vortex. The extra buoyancy, generated by the heat released during combustion, is perhaps an order of magnitude larger than the initial buoyancy of the pure fuel. On the other hand, all four cases had the same initial buoyancy (or the same density difference at the nozzle), and the flame temperature within the burning vortex can be argued to be comparable among the four cases. Thus, the dimensionless parameter $[g(\pi d^2/4) U_0 t^3]^{1/4}/d$ was chosen for scaling of the starting vortex penetration. The theory was appropriate for small density differences and, furthermore, is strictly applicable only to buoyancy-driven flows. One of the implications of the theory is that the above scaling should be free of Reynolds number effects as long as the flow is in the turbulent regime. Moreover, this scaling is applicable only to the burning starting vortex and has no bearing on the stationary portion of the flame.

The tip of the burning starting vortex normalized by the nozzle diameter, Z/d, was plotted against the preceding dimensionless parameter. A least-squares line of the form

$$(Z - Z_0)/d = k\left[g(\pi d^2/4) U_0 t^3\right]^{\frac{1}{4}}/d \qquad (6)$$

was fit to the data, and the calculated correlation coefficients ($\geq$99%) were better than those for the linear fit discussed earlier. As mentioned previously, the relatively short lifetime of the burning vortex does allow a certain flexibility in the power law. Sample plots of Z/d against $[g(\pi d^2/4) U_0 t^3]^{1/4}/d$ are shown in Fig. 6 for all four cases. The data in these plots represent four individual runs corresponding to the data in Fig. 5. Note the consistently larger slope of the least-squares lines for cases 3 and 4 compared to cases 1 and 2, even though the two paired cases had nearly equal initial Reynolds numbers. Fully momentum-driven flames (not addressed in the present experiments) would likely result in a different power law.

The mean values of virtual origin, Z_0/d, found through the least-squares procedure, is listed in Table 3 along with the proportionality constant k. This parameter, which was defined in Eq. (6), is independent, to within the accuracy of the measurements, of the initial Reynolds number for the two values in the current experiments. On the other hand, it appears that the proportionality constant k exhibits a nozzle-diameter dependence even with the starting plume scaling.

There are several possibilities that might explain the observed nozzle-diameter dependence. The mean flame length of the stationary portion of the flow for the larger nozzle was shorter than that for the smaller nozzle by about 25%, implying a slower mixing for the (smaller) 6.4-mm nozzle. One then might also expect a slower mixing rate for the starting vortex from the 6.4-mm nozzle. The slower mixing rate results in a slower decrease of the buoyancy flux, because of mixing with the ambient air, and therefore a faster penetration rate. Although this is a plausible explanation for the observed nozzle-diameter dependence, the reasons for the slower mixing rate with the 6.4-mm nozzle are not known. One potential reason may be the liftoff of the flame above the nozzle observed in several runs with the 6.4-mm nozzle. None of the runs with the 9.9-mm nozzle had lifted flames. The liftoff may play a role in initial formation of the starting vortex and subsequently alter its penetration rate. The observed liftoff with the smaller nozzle is perhaps a consequence of the relatively higher local strain rate at the nozzle exit. Even for the same nozzle Reynolds number associated with the two different nozzle diameters, the larger nozzle velocity of the smaller nozzle increases the strain rate. The higher strain rate of the smaller nozzle would delay combustion and transition to the buoyancy-driven regime. However, it is unclear whether and how this delay could produce consistent changes in the penetration rate within the buoyant regime. Further work is necessary to elucidate the reasons for the different penetration rates observed for the two nozzle diameters.

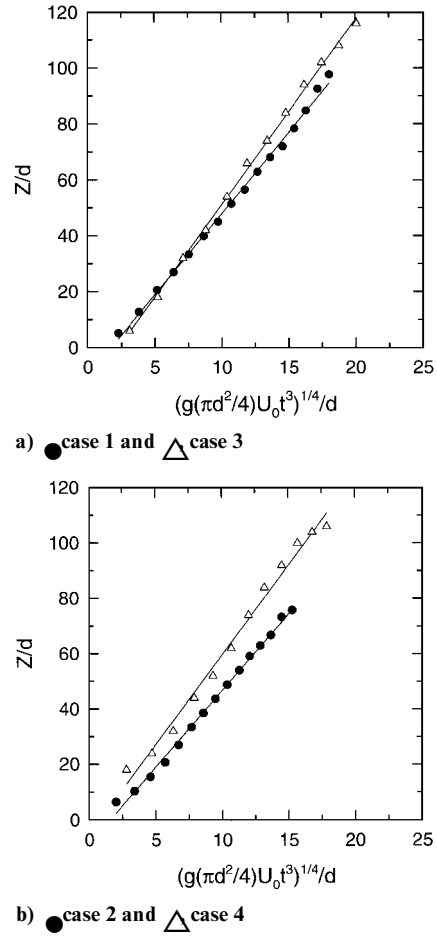

Fig. 6 Penetration of burning vortex as a function of time normalized by the starting plume parameter.

Lateral Spreading

The maximum width δ of the starting vortex was also measured in the present experiments. The spreading rate of turbulent jets normally achieves a constant value, as measured by the rate of increase of the maximum width of the turbulent region. In steady flows, the maximum width increases linearly with the axial extent of the flow. The starting plume is no exception, and the spreading rate of this flow was measured by Turner[17] to be 0.36 ± 0.06. The present data provided the maximum width as a function of time. However, the penetration of the starting vortex with time was available for the same runs from the earlier-reported measurements, thus allowing creation of data sets for the normalized maximum width δ/d as a function of the penetration Z/d. The maximum-width data were fit with least-squares lines having relatively high correlation coefficients, indicating linear spreading, as expected. Sample plots of the maximum width of the starting vortex are presented in Fig. 7 for the runs shown in Fig. 5. The scatter in the data is due to the uneven growth of the starting vortex, as is evident in Fig. 4. The calculated mean spreading rates of $d\delta/dZ$ are reported in Table 3.

The spreading rates do not vary greatly among the four cases. Moreover, the present spreading rates are not the same as those

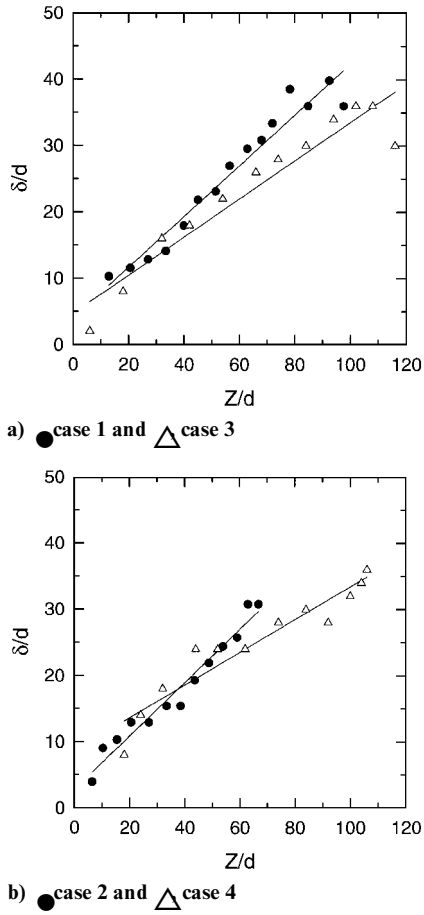

Fig. 7 Maximum width of burning vortex against its penetration.

measured by Turner for the starting plume. In that study, the vertical location of the maximum width was used for calculation of the spreading rate, whereas, in the present calculations, the location of the burning vortex tip was utilized. This was done to avoid introducing errors associated with reading the axial location of maximum width. Assuming that the starting vortex has spherical geometry, Turner's mean spreading rate can be transformed to conform with the present definition. It becomes equal to 0.31 ± 0.05, in agreement with the present values and further validating our use of the starting plume scaling.

Conclusion

The starting vortex of an impulsively generated jet diffusion flame was studied experimentally. The penetration of the burning starting vortex was measured as a function of time for four different flow conditions, covering two nozzle diameters and two initial Reynolds numbers. The stationary diffusion flames were in the buoyancy-driven regime. The penetration of the flame tip associated with the starting vortex could be correlated by a parameter derived from the isothermal, buoyancy-driven starting plume theory of Turner. The starting vortex penetration scales with the nozzle volume flow rate and appears unaffected by the nozzle Reynolds number in the present experiments. An unexplained dependence of penetration on nozzle diameter was observed.

The lateral spreading of the starting vortex was linear with axial distance and the spreading rate was consistent with the previous measurements of starting plumes. The height at which the starting vortex burned off completely was approximately equal to the mean flame length of the stationary flow. The comparable flame lengths indicate that mixing and fuel consumption within the starting vortex are not significantly different from that in the steady flame. The timescale for complete burnoff of the starting vortex at its mean flame height appears to be about one-half of the vortex rotation time at the same location. These findings may be useful in understanding and interpreting the outcome of unsteady combustion processes, especially as it might pertain to active combustion control schemes.

Further experiments on impulsively generated diffusion flames should examine the scaling for penetration of the burning starting vortex in cases where the starting vortex and the stationary jet diffusion flame are fully momentum driven. Such experiments would reveal whether the $t^{1/2}$ scaling, appropriate for the momentum-driven isothermal flows, is applicable to fully momentum-driven impulsively started diffusion flames. On the other hand, flows with even greater buoyancy, which can be achieved by decreasing the nozzle velocity while maintaining a minimum nozzle Reynolds number, should further validate the proposed $t^{3/4}$ scaling for penetration of the starting vortex in diffusion flames.

Acknowledgments

Partial support of this project by a grant from National Science Foundation (CTS-9309321) is greatly appreciated. The image processing software was kindly donated by Data Translation, Inc., of Marlboro, Massachusetts. The authors are grateful to one of the reviewers, who suggested that the initial strain rate affects the liftoff observed with the smaller nozzle.

References

[1]Ho, C.-M., and Huerre, P., "Perturbed Free Shear Layers," *Annual Review of Fluid Mechanics*, Vol. 16, 1984, pp. 365–424.

[2]Crow, S. C., and Champagne, F. H., "Orderly Structure in Jet Turbulence," *Journal of Fluid Mechanics*, Vol. 48, Pt. 3, 1971, pp. 547–591.

[3]Lovett, J. A., and Turns, S. R., "Experiments on Axisymmetrically Pulsed Turbulent Jet Flames," *AIAA Journal*, Vol. 28, No. 1, 1990, pp. 38–46.

[4]Johari, H., and Motevalli, V., "Flame Length Measurements of Burning Fuel Puffs," *Combustion Science and Technology*, Vol. 94, No. 1–6, 1993, pp. 229–244.

[5]Witze, P. O., "The Impulsively-Started Incompressible Turbulent Jet," Sandia Labs., Rept. SAND80-8617, Oct. 1980.

[6]Lahbabi, F. Z., Boree, J., Nuglisch, H. J., and Charnay, G., "Analysis of Starting and Steady Turbulent Jets by Image Processing Techniques," *Third Symposium on Experimental and Numerical Flow Visualization*, FED Vol. 172, American Society of Mechanical Engineers, New York, 1993, pp. 315–321.

[7]Johari, H., Zhang, Q., Rose, M. J., and Bourque, S. M., "Impulsively Started Turbulent Jets," *AIAA Journal*, Vol. 35, No. 4, 1997, pp. 657–662.

[8]Haynes, B. S., and Wagner, H. G., "Soot Formation," *Progress in Energy and Combustion Science*, Vol. 7, 1981, pp. 229–273.

[9]Dahm, W. J. A., and Dimotakis, P. E., "Measurements of Entrainment and Mixing in Turbulent Jets," *AIAA Journal*, Vol. 25, No. 9, 1987, pp. 1216–1223.

[10]Mungal, M. G., Karasso, P. S., and Lozano, A., "The Visible Structure of Turbulent Jet Diffusion Flames: Large-Scale Organization and Flame Tip Oscillation," *Combustion Science and Technology*, Vol. 76, 1991, pp. 165–185.

[11]Peters, N., "Laminar Diffusion Flamelet Models in Non-Premixed Turbulent Combustion," *Progress in Energy and Combustion Science*, Vol. 10, 1984, pp. 319–339.

[12]Cetegen, B. M., and Bogue, D. R., "Combustion in a Stretched Fuel Strip with Finite Rate Chemistry," *Combustion and Flame*, Vol. 86, 1991, pp. 359–370.

[13]Tsuji, H., "Counterflow Diffusion Flames," *Progress in Energy and Combustion Science*, Vol. 8, 1982, pp. 93–119.

[14]Broadwell, J. E., and Breidenthal, R. E., "A Simple Model of Mixing and Chemical Reactions in a Turbulent Shear Layer," *Journal of Fluid Mechanics*, Vol. 125, 1982, pp. 397–410.

[15]Becker, H. A., and Yamazaki, S., "Entrainment, Momentum Flux and Temperature in Vertical Free Turbulent Diffusion Flames," *Combustion and Flame*, Vol. 33, 1978, pp. 123–149.

[16]Becker, H. A., and Liang, D., "Visible Length of Vertical Free Turbulent Diffusion Flames," *Combustion and Flame*, Vol. 32, 1978, pp. 115–137.

[17]Turner, J. S., "The 'Starting Plume' in Neutral Surroundings," *Journal of Fluid Mechanics*, Vol. 13, Pt. 3, 1962, pp. 356–368.

K. Kailasanath
Associate Editor